NEOPLASMA accepted, ahead of print manuscript
Cite article as https://doi.org/10.4149/neo_2026_260408N106

Running title: NSUN2 siRNA & cisplatin promote ferroptosis in CC

NSUN2 siRNA combined with cisplatin promotes ferroptosis and inhibits the proliferation of cervical cancer cells by downregulating GOLPH3 expression

Jun Zhong[1,#], Longnian Hong[1,#], Xiaohua Zhou[1], Guotong Chen[1], Yanting Zou[1], Qiuyu Huang[1], Zhennan Wang[2,*], Hao Huang[1,*]

[1]Department of Gynecology, Affiliated Hospital of Guangdong Medical University, Zhanjiang, Guangdong, China; [2]Department of Oncology, Affiliated Hospital of Guangdong Medical University, Zhanjiang, Guangdong, China

*Correspondence: zhennan@gdmu.edu.cn; hh280080@126.com

[#]Contributed equally to this work.

Received April 8, 2026 / Accepted November 3, 2026

Cisplatin resistance presents a major obstacle to effective treatment of cervical cancer (CC). Inducing ferroptosis represents a promising strategy to overcome cisplatin resistance. Thus, we aim to investigate the regulatory role of GOLPH3 in ferroptosis and its underlying mechanisms.

Gene and protein expression were detected using RT-qPCR and western blot. CCK-8 and colony formation assays were used for cell viability and proliferation measurement. Lipid peroxidation levels were detected using the C11-BODIPY fluorescent probe via flow cytometry, and MDA content was measured by a commercial kit. RIP and MeRIP assays were applied to validate RNA-protein binding and m^5C modification, respectively.

Our results showed that GOLPH3 knockdown enhanced erastin- or cisplatin-induced ferroptosis in CC cells, and GOLPH3 knockdown-induced ferroptosis in cisplatin-treated CC cells was reversed by Fer-1, indicating that GOLPH3 knockdown inhibits cell proliferation via promoting ferroptosis. Besides, GOLPH3 depletion suppressed the AKT/GSK3β/NRF2 pathway, thereby enhancing ferroptosis. Furthermore, NSUN2 mediated m^5C modification of GOLPH3 mRNA and recruited ALYREF to enhance its stability. NSUN2 knockdown downregulated GOLPH3 expression. Furthermore, NSUN2 knockdown augmented cisplatin-induced growth inhibition of parental and cisplatin-resistant CC cells through enhanced ferroptosis, whereas GOLPH3 overexpression reversed this effect.

In conclusion, our findings suggest that NSUN2 may stabilize GOLPH3 mRNA via m^5C modification in an ALYREF-dependent manner, which may activate the AKT/GSK3β/NRF2 pathway to inhibit ferroptosis and potentially contribute to cisplatin resistance in CC.

Key words: NSUN2; GOLPH3; ferroptosis; cisplatin; cervical cancer

Accepted manuscript

Cervical cancer (CC) is a major global threat to women's health, exhibiting high incidence and mortality. Among 36 cancer types, CC ranked 8th in new cases (661,021) and 9th in deaths (348,189), according to global cancer statistics for 2022 [1]. Cisplatin is a commonly used drug for CC that works by damaging the DNA of cancer cells. However, cancer cells can develop resistance to cisplatin, which significantly reduces its effectiveness and may even lead to cancer recurrence, posing a major challenge in current treatment [2]. Ferroptosis is an iron-dependent, programmed cell death modality triggered by the accumulation of lipid peroxidation [3]. Notably, substantial evidence indicated that ferroptosis induction overcame cisplatin resistance in cancers [4], thereby providing a highly promising novel therapeutic direction for cisplatin-resistant CC.

Golgi Phosphoprotein 3 (GOLPH3) is a key regulator of Golgi apparatus function and intracellular transport processes [5]. Its aberrant expression was closely associated with the development, progression, and chemotherapy resistance of various human malignancies [6]. Accumulating evidence indicated that GOLPH3 exerted its oncogenic effects by modulating multiple signaling pathways, thereby promoting tumor cell proliferation, metastasis, and resistance to therapeutic agents [7-9]. For example, GOLPH3 conferred cisplatin resistance in non-small cell lung cancer through elevation of glutathione levels, facilitation of cisplatin efflux, and preservation of the stem cell-like phenotype [7]. Additionally, GOLPH3 was enhanced in CC samples, where it accelerated cell growth and metastasis [8]. In breast cancer, GOLPH3 overexpression enhanced AKT activity, thereby modulating cell cycle-related molecules and promoting tumor cell proliferation and tumorigenesis [9]. Notably, emerging evidence has linked GOLPH3 to ferroptosis regulation. GOLPH3 inhibits ferroptosis in cholangiocarcinoma cells by upregulating SLC7A11 and promotes malignant tumor progression [10]. Moreover, in cisplatin-resistant gastric cancer, Yiqi Huayu Jiedu Tang induced ferroptosis by inactivating the AKT/GSK3β/NRF2 pathway [11]. Based on these observations, it is reasonable to speculate that GOLPH3 knockdown may regulate ferroptosis through the AKT/GSK3β/NRF2 pathway, thereby enhancing the sensitivity of CC cells to cisplatin.

5-methylcytosine (m^5 C), an RNA epigenetic modification where the 5th carbon atom of cytosine undergoes methylation, participates in core processes such as tumor cell proliferation and invasion by regulating the stability, translation efficiency, or localization of target RNAs [12]. NOP2/Sun domain family member 2 (NSUN2), a key RNA methyltransferase mediating m^5 C modification,

Accepted manuscript

regulated oncogenes' and tumor suppressors' abundance to affect cell growth and metastasis of tumor cells across multiple cancer types including CC [13, 14]. Notably, highly expressed NSUN2 stabilized MMP-9 mRNA via m^5 C modification to upregulate its expression, thereby promoting vasculogenic mimicry in CC and resulting in poor patient prognosis [15]. However, whether NSUN2 regulates GOLPH3 expression through m^5 C modification in CC remains unknown. It is noteworthy that m^5 C readers, as key molecules that recognize m^5 C modifications on RNA and govern the fate of target RNAs, play indispensable roles in tumor initiation and progression [16]. Aly/REF export factor (ALYREF) is one of the most extensively studied m^5 C readers. As described in a previous study, ALYREF maintained the stability of PD-L1 mRNA by recognizing NSUN2-mediated m^5 C modifications on it, thereby promoting non-small-cell lung cancer progression and suppressing antitumor immunity [17]. NSUN6 catalyzed the m^5 C modification of NDRG1 mRNA, promoted the binding of the m^5 C reader protein ALYREF to NDRG1 mRNA to enhance its stability, thereby upregulating NDRG1 expression and ultimately leading to radio-resistance in CC [18]. Therefore, we propose that NSUN2 and ALYREF may contribute to CC progression through the regulation of GOLPH3.

Based on the aforementioned evidence, we hypothesize that NSUN2 and ALYREF cooperate to regulate GOLPH3 expression via m^5 C modification, leading to GOLPH3 upregulation, which subsequently activates the AKT/GSK3β/NRF2 signaling pathway and ultimately inhibits ferroptosis in CC cells to confer cisplatin resistance (Figure 1). Notably, combined treatment with siRNA and cisplatin has been verified as an effective combination therapeutic strategy for CC. Existing studies have confirmed that siRNA-mediated gene silencing improved the chemosensitivity of CC cells to cisplatin, and the combined regimen exhibited better anti-tumor effects than cisplatin monotherapy [19]. Consistent with this combination therapy rationale, we reasonably speculate that NSUN2 siRNA can downregulate NSUN2 expression to disrupt the aforementioned regulatory axis, thereby reducing GOLPH3 levels. When combined with cisplatin, NSUN2 siRNA may further augment the suppression of cell viability and proliferation in CC cells by further promoting ferroptosis, potentially reversing cisplatin resistance.

Accepted manuscript

Materials and Methods

Cell culture and treatments. HeLa and SiHa cells, belonging to human cervical cancer cell lines, were obtained from ATCC (USA). SiHa cisplatin-resistant cells were obtained from FENGHUISHENGWU (China). They were cultured in DMEM (Gibco, USA) supplemented with 10% FBS (Gibco) and 1% penicillin-streptomycin mixture (Beyotime, China). Cells were incubated at 37 °C with 5% CO_2 in a humidified incubator.

To induce or inhibit ferroptosis in CC cells, the cells were treated with 10 μM erastin (Selleck Chemicals, USA) or 10 μM ferrostatin-1 (Fer-1, Selleck Chemicals) for 24 h. Next, to determine the optimal concentration of cisplatin, cells were exposed to varying concentrations (0, 0.5, 1, 2, 5, and 10 μg/ml) of cisplatin for 24 h. Additionally, in experiments requiring activation of the AKT/GSK3β/NRF2 pathway, cells were pretreated with 10 μM SC79, an AKT activator, for 1 h.

Cell transfection. Small interfering RNAs targeting GOLPH3 (si-GOLPH3), NSUN2 (si-NSUN2), ALYREF (si-ALYREF) and overexpression plasmids for ALYREF (oe-ALYREF) and GOLPH3 (oe-GOLPH3), along with their controls (si-NC and oe-vector), were obtained from GenePharma (China). The sequence of siRNAs and full cloned sequences of overexpression constructs and schematic diagrams of recombinant plasmids were provided in the supplementary materials. CC cells were plated in 6- well plates overnight and transfected with siRNAs or plasmids using Lipofectamine™ 3000 (Invitrogen, USA) per the manufacturer's protocol for 48 h.

RT-qPCR. Total RNA isolation from CC cells was carried out using TRIzol reagent (Solarbio, China). cDNA synthesis was performed with the reverse transcription kit (Takara, China). Real-time PCR assays were carried out with TB Green® Premix Ex Taq™ (Takara) on a thermal cycler. Gene expression levels were normalized to β-actin, and relative quantification was determined via the $2^{-\Delta\Delta Ct}$ method. Specific primers were synthesized by Sangon Biotech (China) and the sequences were as follows: NSUN2 (F): 5'-TACCCCGAGATCGTCAAGGA-3', NSUN2 (R): 5'-TCAGGATACCTTTTGTAACCAGT-3'; ALYREF (F): 5'-ACAGCAGGCCAAAACAACTT-3', ALYREF (R): 5'-GTGCACGTCTGCTGTTCCTA-3'; GOLPH3 (F): 5'-ACATTAAGCAGCGCCTCATC-3', GOLPH3 (R): 5'-GGTGTTGGCCTTCAGACATT-3'; β-actin (F): 5'-CCCTGGAGAAGAGCTACGAG-3', β-actin (R): 5'-CGTACAGGTCTTTGCGGATG-3'.

Accepted manuscript

Western blot. Proteins of CC cells were isolated via lysis with RIPA buffer (Beyotime), and their concentrations were determined using the BCA assay (Beyotime). For subcellular fractionation, nuclear and cytoplasmic proteins were separated using a commercial kit (Beyotime) following the manufacturer's instructions. Then, proteins were separated by SDS-PAGE electrophoresis and transferred onto a PVDF membrane. The membrane was subjected to blocking treatment with 5% non-fat milk, followed by overnight incubation at 4 °C with the primary antibodies at specific dilutions. Subsequently, the membrane was washed with TBST buffer four times and was incubated with HRP-conjugated secondary antibodies (#31460, #31430, Thermo Fisher Scientific, USA) for 1 h, which was again followed by four washes with TBST. Finally, protein bands were visualized using ECL chemiluminescent reagent (Beyotime), and the images were captured using a BIO-RAD chemiluminescence imaging system. Of note, the information of the primary antibodies was as follows: NSUN2 (#MA5-56501, 1:2000), ALYREF (#PA5-22314, 1:2000), GOLPH3 (#PA5-100010, 1:1000), p-AKT (#44-623G, 1:1000), AKT (#44-609G, 1:1000), p-GSK3β (#MA5-14873, 1:1000), GSK3β (#39-9500, 1:250), NRF2 (#PA5-27882, 1:2000), GPX4 (#MA5-32827, 1:8000), SLC7A11 (#PA1-16893, 1:1000), ACSL4 (#PA5-27137, 1:2000), Cleaved Caspase-3 (#PA5-114687, 1:1000), Bax (#MA5-14003, 1:100), RIP-1 (#PA5-20811, 1:1000), Lamin B1 (#702972, 1:10000) and β-actin (#MA5-15739, 1:5000). All antibodies were purchased from Thermo Fisher Scientific.

CCK-8 assay. Briefly, cells were plated in 96-well culture plates. After the treatments, 10 μl of CCK-8 reagent (Beyotime) was added to each well, followed by incubation at 37 °C for 1 h. Absorbance values for each well were then detected spectrophotometrically at a wavelength of 450 nm.

To explore the combined effects on cell viability, HeLa and SiHa cells were transfected with si-GOLPH3 (0, 0.13, 0.33, 0.66, 1, and 1.33 μg/ml) or si-NSUN2 (0, 0.08, 0.16, 0.32, 0.64, and 0.8 μg/ml) at the indicated concentrations and subsequently treated with a concentration gradient of cisplatin (0, 0.5, 1, 2, 5, and 10 μg/ml) to generate a two-dimensional combination matrix. After 24 h of cisplatin exposure, cell viability was determined using the CCK-8 assay. The resulting cell viability concentration-response data were analyzed using SynergyFinder with the zero-interaction potency (ZIP) model, which evaluates deviations of the observed combination responses from the

Accepted manuscript

expected responses under a non-interaction assumption.

To determine the half-maximal inhibitory concentration (IC_{50}) of cisplatin, cells were treated with gradient concentrations of cisplatin (0, 0.5, 1, 2, 5, 10 μg/ml for HeLa and SiHa cells; 0, 1, 5, 10, 20, 40 μg/ml for SiHa parental cells and cisplatin-resistant cells) for 24 h. The IC_{50} values were calculated by fitting the dose-response curves using nonlinear regression analysis with GraphPad Prism software.

Colony formation assay. CC cells were plated into 6-well plates and cultured for 14 consecutive days. Subsequently, CC cells were fixed with methanol and stained with 0.1% crystal violet. Colony formation was ultimately visualized and recorded as whole-well macroscopic images using a camera (Olympus, Japan).

The measurement of lipid peroxidation. Lipid peroxidation levels were quantitatively assessed using C11-BODIPY (Beyotime) via flow cytometry. C11-BODIPY is a ratiometric probe, and the green/red fluorescence ratio was therefore used to quantify lipid peroxidation. Briefly, CC cells were incubated with C11-BODIPY at 37 °C for 30 min in the dark. After incubation, the cells were washed three times with pre-cooled PBS to remove unbound probe. Subsequently, the stained cells were resuspended in PBS, and mean fluorescence intensity (MFI) in green and red were acquired by flow cytometry (BD Biosciences, USA). The green/red fluorescence ratio was calculated as the ratio of the MFI of the entire cell population for each sample. The ratio obtained from the first group was set as the reference value of 1.00, and the relative lipid peroxidation level of the other groups was normalized accordingly.

Detection of malondialdehyde (MDA) levels. CC cells were lysed and subjected to centrifugation, after which the supernatant was harvested. MDA levels in the resulting cell lysates were quantified using an MDA assay kit (#A003-1-2, Nanjing Jiancheng Bioengineering Institute, China) following the manufacturer's instructions.

Measurements of iron concentration. According to the manufacturer's instructions, ferrous (Fe^{2+}), and ferric (Fe^{3+}) ions were quantified using an iron assay kit (#ab83366, Abcam, UK).

Bioinformatic analysis. Bioinformatic analyses were performed using publicly available databases. The starBase database (http://starbase.sysu.edu.cn/) was employed to analyze the correlation between NSUN2 and GOLPH3 expression in cervical squamous cell carcinoma and endocervical

Accepted manuscript

adenocarcinoma (CESC), as well as to identify potential RNA-binding proteins (RBPs) of GOLPH3. The RNAm5Cfinder database (http://www.rnam5cfinder.com/) was utilized to predict potential m^5 C modification sites within the GOLPH3 mRNA sequence.

Methylated RNA Immunoprecipitation (MeRIP) assay. The m^5 C RNA methylation levels were assessed following the manufacturer's instructions for the Magna RIP kit (Millipore, USA). CC cells were plated in 6-well plates and collected 24 h after seeding. Total RNA was isolated with TRIzol reagent (Invitrogen), then subjected to immunoprecipitation using magnetic beads conjugated with m^5 C-specific antibody (#MA5-24694, Thermo Fisher Scientific) or IgG antibody (#MA5-56524, Thermo Fisher Scientific). The immunoprecipitated methylated RNA was subsequently purified, and RT- qPCR was performed to evaluate m^5 C methylation of GOLPH3 mRNA.

RNA immunoprecipitation (RIP) assay. The interactions between NSUN2 and GOLPH3 mRNA as well as ALYREF and GOLPH3 mRNA were evaluated by RIP using a commercial RIP assay kit (Beyotime). Briefly, CC cells were lysed in RIP lysis buffer. After centrifugation, the supernatant was collected. Protein A/G magnetic beads were prepared by suspension in RIP wash buffer and conjugated with anti-NSUN2 (#MA5-56501, Thermo Fisher Scientific), anti-ALYREF (#PA5-22314, Thermo Fisher Scientific) or control anti-IgG (#MA5-56524, Thermo Fisher Scientific) for 1 h at 4 °C. The cell lysate was then incubated with the antibody-bound beads overnight at 4 °C. Immunoprecipitated complexes were isolated following the kit instructions. Enrichment of anti-NSUN2 or anti-ALYREF-associated RNA was subsequently quantified by RT-qPCR.

RNA stability assay. GOLPH3 mRNA stability in CC cells was evaluated following transcriptional inhibition with Actinomycin D (5 μg/ml, Merck, Germany). GOLPH3 mRNA abundance was measured via RT-qPCR at specified time points (0, 2 and 4 h) after Actinomycin D treatment.

Statistical analysis. Data were presented as mean±standard deviation (SD) of three independent biological replicates. Statistical analyses were performed using GraphPad Prism 9. Group comparisons were made using Student's t-test (for two groups) or one-way ANOVA followed by Tukey's post-hoc test (for three or more groups). Differences were considered statistically significant at $p < 0.05$.

Accepted manuscript

Results

GOLPH3 siRNA augmented cisplatin-induced growth inhibition in CC cells by enhancing ferroptosis. To investigate whether GOLPH3 knockdown promotes ferroptosis in CC cells, we transfected HeLa and SiHa cells with si-GOLPH3 or control si-NC and found that si-GOLPH3 transfection downregulated GOLPH3 expression in CC cells (Figures 2A, 2B). To exclude the possibility that GOLPH3 knockdown induces apoptosis or necrosis, we also analyzed the expression of apoptotic markers Cleaved Caspase-3 and Bax, as well as the necrotic marker RIP-1. No significant differences in these protein levels were observed between the si-GOLPH3+cisplatin and si-NC+cisplatin groups, indicating that GOLPH3 knockdown may not affect cisplatin-induced apoptosis or necrosis (Supplementary Figure S1). Then, HeLa and SiHa cells were transfected with si-GOLPH3 or control si-NC, followed by erastin (a ferroptosis inducer) treatment. As shown in Figures 2C-2F, erastin could inhibit cell viability and proliferation and increase lipid peroxidation levels and MDA content. However, GOLPH3 knockdown further enhanced these erastin-induced changes. These results indicated that GOLPH3 knockdown inhibited CC cell growth by promoting ferroptosis. Subsequently, we explored whether si-GOLPH3 and cisplatin could cooperatively promote ferroptosis, thereby further inhibiting CC cell proliferation. First, the effects of cisplatin at varying concentrations (0, 0.5, 1, 2, 5, 10 μg/ml), either alone or combined with si-GOLPH3, on CC cells were evaluated. We observed that cisplatin suppressed cell viability in a dose-dependent pattern, and GOLPH3 knockdown enhanced this inhibitory effect (Figure 2G). SynergyFinder analysis further revealed that the ZIP synergy scores across all treatment pairs were 14.976 for HeLa cells and 14.338 for SiHa cells (Supplementary Figure S2A), indicating a synergistic interaction. Based on the CCK-8 results, SiHa cells were treated with 10 μg/ml cisplatin, while HeLa cells received a 5 μg/ml cisplatin treatment for subsequent experiments. Further experiments revealed that GOLPH3 siRNA treatment inhibited the proliferation and increased lipid peroxidation and MDA levels in cisplatin-induced CC cells (Figures 2H-2J). To further confirm that the enhanced antitumor effect of si-GOLPH3 combined with cisplatin was specifically mediated by ferroptosis, si-GOLPH3-transfected CC cells were treated with cisplatin in the presence or absence of Fer-1, a ferroptosis inhibitor. As shown in Supplementary Figures S3A-S3D, si-GOLPH3-induced reduction

Accepted manuscript

in cell viability, along with the increased levels of lipid peroxidation, MDA content, and the Fe^{2+} /Fe^{3+} ratio, were all reversed by Fer-1 co-treatment. Additionally, GOLPH3 knockdown upregulated the expression of ACSL4, while downregulating GPX4 and SLC7A11 in cisplatin-treated cells; these protein-level changes were also effectively counteracted by Fer-1 administration (Supplementary Figure S3E). Taken together, GOLPH3 siRNA and cisplatin cooperatively promoted ferroptosis, leading to an inhibition of CC cell growth.

GOLPH3 knockdown increased ferroptosis in CC cells by suppressing the AKT/GSK3β/NRF2 pathway. To explore whether GOLPH3 regulates ferroptosis in CC cells by modulating the AKT/GSK3β/NRF2 pathway, HeLa and SiHa cells were transfected with si-GOLPH3 or si-NC, respectively. Results showed that GOLPH3 knockdown reduced the ratios of p-AKT/AKT and p-GSK3β/GSK3β, as well as NRF2 level (Figure 3A). To further examine the effects of GOLPH3 on the nuclear-cytoplasmic distribution of NRF2, HeLa and SiHa cells were subjected to si-GOLPH3 or oe-GOLPH3 transfection. GOLPH3 knockdown reduced the abundance of NRF2 protein in the nucleus, with no obvious change in the cytoplasm, whereas GOLPH3 overexpression increased the abundance of NRF2 protein in the nucleus (Figure 3B). Subsequently, pretreatment of si-GOLPH3-transfected cells with the AKT activator SC79 successfully restored the decreased p-AKT/AKT ratio (Figure 3C). Furthermore, after subsequent treatment with the ferroptosis inducer erastin, GOLPH3 knockdown inhibited the viability and proliferation of erastin-induced CC cells, while SC79 treatment reversed this effect (Figures 3D, 3E). Meanwhile, GOLPH3 knockdown promoted lipid peroxidation levels and MDA accumulation in erastin-induced CC cells, and these changes were also reversed by SC79 treatment (Figures 3F, 3G). Collectively, GOLPH3 knockdown enhanced ferroptosis in CC cells by inhibiting the AKT/GSK3β/NRF2 pathway.

NSUN2 mediated the m^5 C modification of GOLPH3 and increased its stability. Notably, starBase database analysis revealed a positive linear relationship between NSUN2 and GOLPH3 expression in CESC (Figure 4A). Additionally, RNAm5Cfinder database revealed that GOLPH3 mRNA contains potential m^5 C modification sites. Subsequent MeRIP assays in HeLa and SiHa cells confirmed obvious m^5 C modification on GOLPH3 mRNA (Figure 4B), and RIP assay further verified that NSUN2 bound to GOLPH3 mRNA (Figure 4C). To clarify the regulatory role of NSUN2 in GOLPH3 expression, we transfected CC cells with si-NSUN2 for gene knockdown, and

Accepted manuscript

the results showed that NSUN2 knockdown reduced both NSUN2 and GOLPH3 mRNA and protein levels (Figures 4D, 4E). MeRIP assay indicated that it could significantly reduce the m^5C modification level of GOLPH3 mRNA (Figure 4F). In addition, detection of mRNA stability after transcription blockage with Actinomycin D revealed that NSUN2 knockdown promoted the degradation of GOLPH3 mRNA (Figure 4G). Collectively, NSUN2 enhanced GOLPH3 mRNA stability by mediating its m^5C modification, thereby positively regulating GOLPH3 expression.

ALYREF was implicated in the NSUN2-mediated GOLPH3 mRNA stability. Of note, starBase database identified ALYREF as a potential RNA-binding protein (RBP) of GOLPH3. To probe whether ALYREF contributes to NSUN2-mediated regulation of GOLPH3 mRNA stability, we confirmed through RIP assay that ALYREF bound to GOLPH3 mRNA (Figure 5A). Subsequently, ALYREF was knocked down using si-ALYREF in HeLa and SiHa cells, and the results showed that ALYREF knockdown reduced GOLPH3 expression (Figures 5B, 5C) and promoted GOLPH3 mRNA degradation (Figure 5D). To further clarify the roles of ALYREF and NSUN2 in regulating GOLPH3 expression, CC cells were transfected with si-NSUN2 alone, oe-ALYREF alone, or a combination of both. In the presence of NSUN2, ALYREF overexpression increased the level of GOLPH3. However, under the condition of NSUN2 knockdown, the promotional effect of ALYREF overexpression on GOLPH3 expression was diminished (Figures 5E, 5F). Following transfection and Actinomycin D treatment, we found that ALYREF overexpression stabilized GOLPH3 mRNA when NSUN2 was present. This stabilizing effect was weakened upon NSUN2 knockdown (Figure 5G). Collectively, these findings indicated that ALYREF was implicated in NSUN2-mediated regulation of GOLPH3 mRNA stability and its expression.

The combination of NSUN2 siRNA and cisplatin inhibited CC cell growth by enhancing ferroptosis via GOLPH3 suppression. We delivered si-NSUN2 alone or co-delivered si-NSUN2 and oe-GOLPH3 into HeLa and SiHa cells, respectively. Results showed that si-NSUN2 treatment reduced NSUN2 and GOLPH3 levels, while GOLPH3 overexpression effectively restored GOLPH3 expression without obviously affecting NSUN2 expression (Figure 6A). Subsequently, CC cells in each group were treated with cisplatin. Compared with the cisplatin monotherapy, si-NSUN2 combined with cisplatin amplified cisplatin-induced suppression of CC cell viability and proliferation, an effect abolished by GOLPH3 overexpression (Figures 6B, 6C). To evaluate the

Accepted manuscript

combined effects of si-NSUN2 and cisplatin, CC cells were transfected with varying concentrations of si-NSUN2 and subsequently treated with different concentrations of cisplatin. SynergyFinder analysis further revealed that the ZIP synergy scores across all treatment pairs were 13.97 for HeLa cells and 12.772 for SiHa cells (Supplementary Figure S2B), indicating a synergistic interaction. Regarding ferroptosis-related indicators, si-NSUN2 combined with cisplatin treatment increased cellular lipid peroxidation levels and MDA content, and GOLPH3 overexpression effectively abolished the abnormal changes of these indicators (Figures 6D, 6E). Collectively, si-NSUN2 enhanced cisplatin-associated growth inhibition and increased ferroptosis-related changes in CC cells.

NSUN2 knockdown resensitized SiHa cisplatin-resistant cells to cisplatin by suppressing GOLPH3 and promoting ferroptosis. To evaluate the drug resistance characteristics of SiHa cisplatin-resistant cells, we first compared the responses of parental and resistant cells to gradient concentrations of cisplatin (0, 1, 5, 10, 20, 40 μg/ml). The results showed that the IC_{50} value of resistant cells (43.46 μg/ml) was higher than that of parental cells (11.87 μg/ml) (Supplementary Figure S4A), confirming a stable drug-resistant phenotype. Subsequently, we transfected SiHa cisplatin-resistant cells with si-NSUN2 or co-transfected with si-NSUN2 and oe-GOLPH3. The results demonstrated that si-NSUN2 effectively downregulated both NSUN2 and GOLPH3 protein levels, whereas GOLPH3 overexpression specifically restored GOLPH3 expression without markedly affecting NSUN2 levels (Supplementary Figure S4B). On this basis, gradient concentrations of cisplatin were applied to each transfected group, and the results revealed that NSUN2 knockdown enhanced the sensitivity of resistant cells to cisplatin, while GOLPH3 overexpression partially reversed this sensitizing effect (Supplementary Figure S4C). Furthermore, NSUN2 knockdown markedly inhibited colony formation and elevated lipid peroxidation and MDA levels; conversely, GOLPH3 overexpression effectively alleviated the reduction in colony formation (Supplementary Figure S4D) and the increases in lipid peroxidation (Supplementary Figure S4E) and MDA levels (Supplementary Figure S4F). Collectively, in SiHa cisplatin-resistant cells, targeting NSUN2 restored cisplatin sensitivity by enhancing ferroptosis through downregulation of GOLPH3.

Accepted manuscript

Discussion

Cisplatin resistance poses a major obstacle in the clinical management of CC, often leading to therapeutic failure and disease recurrence [20]. Ferroptosis has emerged as a promising therapeutic vulnerability that may be exploited to overcome chemoresistance [21]. However, the molecular mechanisms linking ferroptosis regulation to cisplatin resistance in CC remain incompletely understood. Our findings suggested that the NSUN2/ALYREF-mediated m^5C modification stabilized GOLPH3 mRNA, which subsequently activated the AKT/GSK3β/NRF2 signaling pathway to suppress ferroptosis and confer cisplatin resistance. In recent years, numerous studies have focused on exploring strategies to improve cisplatin susceptibility in cervical cancer cells, with combination therapy emerging as a well-documented effective approach [19, 22]. For instance, the combination of baicalein and cisplatin promoted copper ion accumulation via the Akt pathway, thereby enhancing cisplatin susceptibility of CC cells [22]. Additionally, the combination of cisplatin with HPV E6/E7-siRNAs induced apoptosis of CC cells, achieving the effect of improving cisplatin sensitivity [19]. In our study, targeted disruption of this regulatory axis through NSUN2 knockdown augmented cisplatin-induced ferroptosis and growth inhibition of CC cells.

GOLPH3 has emerged as a critical oncogenic regulator in multiple malignancies [8, 23]. For instance, elevated GOLPH3 expression contributed to CC progression by activating the Wnt/β-catenin pathway [8]. Consistently, our study found that GOLPH3 knockdown attenuated CC cell viability and proliferation. Besides, GOLPH3 played a ferroptosis-related role in cancers [10, 24]. In colorectal cancer, it inhibited ferroptosis by inducing PHB1/PHB2 expression and interacting with PHB2/NRF2, thereby promoting tumor cell survival [24]. Similarly, in cholangiocarcinoma, GOLPH3 was highly expressed and correlated with poor prognosis and it facilitated SLC7A11 expression to suppress ferroptosis and promote tumor progression [10]. We further confirmed the involvement of GOLPH3 in ferroptosis regulation in CC, showing that GOLPH3 knockdown promoted erastin-induced ferroptosis in CC cells. Besides, ferroptosis inhibitor Fer-1 suppressed the antitumor activity induced by GOLPH3 knockdown. Of note, inducing ferroptosis has been shown to effectively reverse tumor cell resistance to cisplatin [25, 26]. For example, in CC, high expression of NDUFA8 suppressed ferroptosis, leading to cisplatin resistance [26]. Meanwhile, elevated SLC25A10 enhanced GPX4 expression, which inhibited

Accepted manuscript

365 ferroptosis and similarly conferred cisplatin resistance [25]. In our study, we observed that
366 GOLPH3 knockdown promoted ferroptosis in cisplatin-treated CC cells. Notably, the
367 AKT/GSK3β/NRF2 pathway is a key axis regulating cellular antioxidant stress response and it is
368 frequently hyperactivated in tumors, promoting tumor survival by enhancing antioxidant capacity,
369 chemotherapy resistance, and malignant progression [11, 27]. GOLPH3 overexpression activated
370 Akt, which further regulated the Wnt signaling pathway via GSK3β to promote proliferation and
371 inhibit apoptosis in colon cancer cells [28]. Here, GOLPH3 knockdown promoted ferroptosis in CC
372 cells by suppressing the AKT/GSK3β/NRF2 pathway, and this effect was reversed by the AKT
373 activator SC79.
374 The m^5 C RNA modification, dynamically regulated by writers, readers, and erasers, forms distinct
375 regulatory networks across different tumors, influencing tumor progression, metastasis, immune
376 evasion, and chemoresistance [29]. The RNAm5Cfinder database predicted that the mRNA of
377 GOLPH3 contained potential m^5 C modification sites, indicating that GOLPH3 expression could be
378 regulated by m^5 C modification in CC. The m^5 C modification of target genes relies on the
379 coordinated involvement of writers and readers, among which NSUN2 is a widely reported writer
380 and ALYREF serves as a classic reader in this modification process [30, 31]. More importantly,
381 starBase database predicted a positive correlation between NSUN2 and GOLPH3 expression in
382 CESC. Besides, starBase database revealed that ALYREF could interact with GOLPH3 mRNA. As
383 documented previously, in colorectal cancer, NSUN2 and ALYREF cooperated to enhance the
384 mRNA stability and expression of PHGDH, thereby regulating intracellular ROS levels and
385 apoptosis, and ultimately promoting disease progression [32]. NSUN2 mediated the m^5 C
386 modification of PFAS, which was recognized by ALYREF to enhance PFAS mRNA stability and
387 expression, thereby regulating purine biosynthesis and promoting the development of
388 retinoblastoma [33]. In current study, we demonstrated that the writer protein NSUN2 mediated the
389 m^5 C modification of GOLPH3 mRNA and recruited the reader protein ALYREF, which together
390 enhanced GOLPH3 mRNA stability and expression in CC. Ultimately, knocking down NSUN2
391 enhanced cisplatin-induced ferroptosis in both parental and resistant CC cells by suppressing
392 GOLPH3, thereby augmenting the inhibition of cancer cell growth.
393 In conclusion, this study suggested a potential mechanism by which NSUN2/ALYREF-mediated

Accepted manuscript

m^5 C modification may inhibit ferroptosis through stabilizing GOLPH3 mRNA and activating the AKT/GSK3β/NRF2 pathway, thereby potentially contributing to cisplatin resistance in CC. Additionally, si-NSUN2 combined with cisplatin enhanced ferroptosis and significantly suppressed cell growth *in vitro*, which warrants further validation as a potential novel combination therapeutic strategy for overcoming cisplatin resistance. However, this study has certain limitations. Firstly, all experimental data in this study were derived from conventional HeLa, SiHa cell lines and SiHa cisplatin-resistant cell lines. Given the absence of validation in clinical patient-derived samples and *in vivo* xenograft models, our conclusions remain preliminary and the translational potential of these findings is limited. Besides, the complexity of the m^5 C modification regulatory network suggests that other writer or reader proteins may be involved in the post-transcriptional regulation of GOLPH3, which awaits systematic screening.

deviation

Acknowledgements: This work was supported by Guangdong Provincial Medical Science and Technology Research Fund Project (No. B2022111).

Supplementary data are available in the online version of the paper.

References

[1] BRAY F, LAVERSANNE M, SUNG H, FERLAY J, SIEGEL RL et al. Global cancer statistics 2022: GLOBOCAN estimates of incidence and mortality worldwide for 36 cancers in 185 countries. CA Cancer J Clin 2024; 74: 229-263. https://doi.org/10.3322/caac.21834

[2] ZHANG L, LIU W, LI Y, FU Y, XU C et al. Polyphyllin I Sensitizes Cisplatin-Resistant Human Cervical Cancer Cells to Cisplatin Treatment. Nutr Cancer 2024; 76: 656-665. https://doi.org/10.1080/01635581.2024.2350107

[3] ZHOU Q, MENG Y, LI D, YAO L, LE J et al. Ferroptosis in cancer: From molecular mechanisms to therapeutic strategies. Signal Transduct Target Ther 2024; 9: 55. https://doi.org/10.1038/s41392-024-01769-5

[4] WANG X, DU Q, MAI Q, ZOU Q, WANG S et al. Targeting FASN enhances cisplatin sensitivity via SLC7A11-mediated ferroptosis in cervical cancer. Transl Oncol 2025; 56: 102396. https://doi.org/10.1016/j.tranon.2025.102396

Accepted manuscript

[5] LI T, YOU H, ZHANG J, MO X, HE W et al. Study of GOLPH3: a potential stress-inducible protein from Golgi apparatus. Mol Neurobiol 2014; 49: 1449-1459. https://doi.org/10.1007/s12035-013-8624-2

[6] SECHI S, FRAPPAOLO A, KARIMPOUR-GHAHNAVIEH A, PIERGENTILI R, GIANSANTI MG. Oncogenic Roles of GOLPH3 in the Physiopathology of Cancer. Int J Mol Sci 2020; 21: 933. https://doi.org/10.3390/ijms21030933

[7] WEI Q, LIN J, LIN Z, YU N, WU Y et al. GOLPH3 inhibition overcomes cisplatin resistance by restoring the glutathione/reactive oxygen species balance in the A549 non- small cell lung cancer cell line. Oncol Rep 2024; 52: 170. https://doi.org/10.3892/or.2024.8829

[8] YANG H, MA X, SONG B, WANG D, CHAI Z. Golgi Phosphoprotein 3 Promotes Cervical Cancer Progression via Wnt/β-catenin Mediated Epithelial-Mesenchymal Transition. Ann Clin Lab Sci. 2023; 53: 738-748.

[9] ZENG Z, LIN H, ZHAO X, LIU G, WANG X et al. Overexpression of GOLPH3 promotes proliferation and tumorigenicity in breast cancer via suppression of the FOXO1 transcription factor. Clin Cancer Res 2012; 18: 4059-4069. https://doi.org/10.1158/1078-0432.CCR-11-3156

[10] YIN Z, LIU Q, GAO Y, WANG R, QI Y et al. GOLPH3 promotes tumor malignancy via inhibition of ferroptosis by upregulating SLC7A11 in cholangiocarcinoma. Mol Carcinog 2024; 63: 912-925. https://doi.org/10.1002/mc.23697

[11] HUANG W, WEN F, YANG P, LI Y, LI Q et al. Yi-qi-hua-yu-jie-du decoction induces ferroptosis in cisplatin-resistant gastric cancer via the AKT/GSK3β/NRF2/GPX4 axis. Phytomedicine 2024; 123: 155220. https://doi.org/10.1016/j.phymed.2023.155220

[12] YU L, XU H, XIONG H, YANG C, WU Y et al. The role of m5C RNA modification in cancer development and therapy. Heliyon 2024; 10: e38660. https://doi.org/10.1016/j.heliyon.2024.e38660

[13] CHEN Y, ZUO X, WEI Q, XU J, LIU X et al. Upregulation of LRRC8A by m(5)C modification-mediated mRNA stability suppresses apoptosis and facilitates tumorigenesis in cervical cancer. Int J Biol Sci 2023; 19: 691-704. https://doi.org/10.7150/ijbs.79205

[14] LI P, HUANG D. NSUN2-mediated RNA methylation: Molecular mechanisms and clinical relevance in cancer. Cell Signal 2024; 123: 111375. https://doi.org/10.1016/j.cellsig.2024.111375

[15] LUO J, LI G, YE M, XU X, QI M et al. RNA methyltransferase NSUN2 enhances vasculogenic mimicry and malignant progression of cervical cancer through upregulation of MMP-9. Oncol Lett 2026; 31: 165. https://doi.org/10.3892/ol.2026.15518

[16] ZHAO T, ZHANG Z, CHEN Z, XU G, WANG Y et al. Biological functions of 5-methylcytosine RNA-binding proteins and their potential mechanisms in human cancers. Front Oncol 2025; 15: 1534948. https://doi.org/10.3389/fonc.2025.1534948

[17] YANG Y, CAO L, XU X, LI D, DENG Y et al. NSUN2/ALYREF axis-driven m(5)C methylation enhances PD-L1 expression and facilitates immune evasion in non-small-cell lung cancer. Cancer Immunol Immunother 2025; 74: 132. https://doi.org/10.1007/s00262-025-03986-5

Accepted manuscript

[18] YU M, NI M, XU F, LIU C, CHEN L et al. NSUN6-mediated 5-methylcytosine modification of NDRG1 mRNA promotes radioresistance in cervical cancer. Mol Cancer 2024; 23: 139. https://doi.org/10.1186/s12943-024-02055-2

[19] JUNG HS, ERKIN OC, KWON MJ, KIM SH, JUNG JI et al. The synergistic therapeutic effect of cisplatin with Human papillomavirus E6/E7 short interfering RNA on cervical cancer cell lines in vitro and in vivo. Int J Cancer 2012; 130: 1925-1936. https://doi.org/10.1002/ijc.26197

[20] BHATTACHARJEE R, DEY T, KUMAR L, KAR S, SARKAR R et al. Cellular landscaping of cisplatin resistance in cervical cancer. Biomed Pharmacother 2022; 153: 113345. https://doi.org/10.1016/j.biopha.2022.113345

[21] ZHONG S, WANG Z, YANG J, JIANG D, WANG K. Ferroptosis-related oxaliplatin resistance in multiple cancers: Potential roles and therapeutic Implications. Heliyon 2024; 10: e37613. https://doi.org/10.1016/j.heliyon.2024.e37613

[22] JIN Y, WU Q, PAN S, ZHOU Q, LIU H et al. Baicalein enhances cisplatin sensitivity in cervical cancer cells by promoting cuproptosis through the Akt pathway. Biomed Pharmacother 2024; 179: 117415. https://doi.org/10.1016/j.biopha.2024.117415

[23] FRAPPAOLO A, ZACCAGNINI G, GIANSANTI MG. GOLPH3-mTOR Crosstalk and Glycosylation: A Molecular Driver of Cancer Progression. Cells 2025; 14: 439. https://doi.org/10.3390/cells14060439

[24] CHEN L, WANG C, CHEN X, WU Y, CHEN M et al. GOLPH3 inhibits erastin-induced ferroptosis in colorectal cancer cells. Cell Biol Int 2024; 48: 1198-1211. https://doi.org/10.1002/cbin.12190

[25] MA C, LU X, NI C, GAO Y, YANG F et al. SLC25A10 promotes cisplatin resistance by inhibiting ferroptosis in cervical cancer. Cell Death Discov 2025; 11: 447. https://doi.org/10.1038/s41420-025-02712-5

[26] XIANG H, SUN J, KONG L, WANG Y, QIU X et al. NDUFA8 promotes cell viability and inhibits ferroptosis and cisplatin sensitivity by stabilizing Fe-S clusters in cervical cancer. Naunyn Schmiedebergs Arch Pharmacol 2025; 398: 15547-15559. https://doi.org/10.1007/s00210-025-04237-1

[27] SEN U, COLEMAN C, GANDHI N, JETHALIA V, DEMIRCIOGLU D et al. SCD1 Inhibition Blocks the AKT-NRF2-SLC7A11 Pathway to Induce Lipid Metabolism Remodeling and Ferroptosis Priming in Lung Adenocarcinoma. Cancer Res 2025; 85: 2485-2503. https://doi.org/10.1158/0008-5472.CAN-24-2745

[28] QIU CZ, WANG MZ, YU WS, GUO YT, WANG CX et al. Correlation of GOLPH3 Gene with Wnt Signaling Pathway in Human Colon Cancer Cells. J Cancer 2016; 7: 928-934. https://doi.org/10.7150/jca.13968

[29] ZHANG L, LI Y, LI L, YAO F, CAI M et al. Detection, molecular function and mechanisms of m5C in cancer. Clin Transl Med 2025; 15: e70239. https://doi.org/10.1002/ctm2.70239

[30] HU X, DING C, LU J, LI J, REN X et al. RNA-m5C regulatory atlas of human fetal tissues uncover the activities of Nsun2/Jarid2/Alyref axis. J Adv Res 2026; 83: 659-676. https://doi.org/10.1016/j.jare.2025.08.004

[31] SONG H, ZHANG J, LIU B, XU J, CAI B et al. Biological roles of RNA m(5)C modification and its implications in Cancer immunotherapy. Biomark Res 2022; 10: 15. https://doi.org/10.1186/s40364-022-00362-8

Accepted manuscript

[32] LI H, GONG T, ZHAO Y, LUO Y, TANG S et al. NSUN2 promotes colorectal cancer progression by stabilizing PHGDH mRNA to promote serine metabolism reprogramming. Cancer Metab 2025; 13: 37. https://doi.org/10.1186/s40170-025-00406-1

[33] ZUO S, LI L, WEN X, GU X, ZHUANG A et al. NSUN2-mediated m(5) C RNA methylation dictates retinoblastoma progression through promoting PFAS mRNA stability and expression. Clin Transl Med 2023; 13: e1273. https://doi.org/10.1002/ctm2.1273

Figure Legends

Figure 1. Graphical abstract. NSUN2 and ALYREF cooperate to regulate GOLPH3 expression via m^5C modification, leading to GOLPH3 upregulation, which subsequently activates the AKT/GSK3β/NRF2 signaling pathway and ultimately inhibits ferroptosis in CC cells to confer cisplatin resistance.

Figure 2. GOLPH3 siRNA augmented cisplatin-induced growth inhibition in CC cells by enhancing ferroptosis. HeLa and SiHa cells were transfected with si-NC or si-GOLPH3 for 48 h. A, B) GOLPH3 levels were detected by RT-qPCR and western blot, respectively. For GOLPH3 mRNA, si-NC vs. si-GOLPH3: p=0.0043 (HeLa) and p=0.0011 (SiHa); for GOLPH3 protein, si-NC vs. si-GOLPH3: p=0.0175 (HeLa) and p=0.0042 (SiHa). The transfected cells were treated with 10 μM erastin for 24 h. C) Cell viability was assessed by CCK-8 assay. For HeLa, Control vs. Control+erastin: p=0.0007; si-NC+erastin vs. si-GOLPH3+erastin: p=0.0455; for SiHa, Control vs. Control+erastin: p=0.0011; si-NC+erastin vs. si-GOLPH3+erastin: p=0.0336. D) Cell proliferation was measured by colony formation assay. For HeLa, Control vs. Control+erastin: p=0.0005; si-NC+erastin vs. si-GOLPH3+erastin: p=0.0061; for SiHa, Control vs. Control+erastin: p=0.0038; si-NC+erastin vs. si-GOLPH3+erastin: p=0.0024. E) Lipid peroxidation levels were detected using C11-BODIPY fluorescent probe via flow cytometry. For HeLa, Control vs. Control+erastin: p=0.0002; si-NC+erastin vs. si-GOLPH3+erastin: p=0.0349; for SiHa, Control vs. Control+erastin: p=0.0036; si-NC+erastin vs. si-GOLPH3+erastin: p=0.0003. F) MDA content was measured by commercial assay kit. For HeLa, Control vs. Control+erastin: $p < 0.0001$; si-NC+erastin vs. si-GOLPH3+erastin: p=0.0051; for SiHa, Control vs. Control+erastin: p=0.0011; si-NC+erastin vs. si-GOLPH3+erastin: p=0.0085. The transfected cells were treated with the indicated concentrations of cisplatin (0, 0.5, 1, 2, 5, 10 μg/ml) for 24 h. G) Cell viability following treatment with increasing

Accepted manuscript

concentrations of cisplatin was assessed by CCK-8 assay. For HeLa, si-NC+cisplatin vs. si-GOLPH3+cisplatin: p=0.0024; for SiHa, si-NC+cisplatin vs. si-GOLPH3+cisplatin: p=0.0019. The transfected cells were treated with 5 μg/ml cisplatin (HeLa) or 10 μg/ml cisplatin (SiHa), for 24 h. H) Cell proliferation was measured by colony formation assay. For HeLa, si-NC+cisplatin vs. si-GOLPH3+cisplatin: p=0.0068; for SiHa, si-NC+cisplatin vs. si-GOLPH3+cisplatin: $p < 0.0001$. I) Lipid peroxidation levels were detected using C11-BODIPY fluorescent probe via flow cytometry. For HeLa, si-NC+cisplatin vs. si-GOLPH3+cisplatin: p=0.0009; for SiHa, si-NC+cisplatin vs. si-GOLPH3+cisplatin: p=0.0017. J) MDA content was measured by commercial kit. For HeLa, si-NC+cisplatin vs. si-GOLPH3+cisplatin: p=0.0082; for SiHa, si-NC+cisplatin vs. si-GOLPH3+cisplatin: p=0.0054. All experiments were conducted in three independent biological replicates. n=3. *$p < 0.05$, **$p < 0.01$, ***$p < 0.001$

Figure 3. GOLPH3 knockdown increased ferroptosis in CC cells by suppressing the AKT/GSK3β/NRF2 pathway. HeLa and SiHa cells were transfected with si-NC or si-GOLPH3 for 48 h. A) The protein levels of p-AKT, AKT, p-GSK3β, GSK3β, and NRF2 were determined by western blot. For p-AKT/AKT si-NC vs. si-GOLPH3: p=0.0083 (HeLa) and p=0.0015 (SiHa); For p-GSK3β/GSK3β: si-NC vs. si-GOLPH3: p=0.0008 (HeLa) and p=0.0089 (SiHa); for total NRF2: si-NC vs. si-GOLPH3: $p < 0.0001$ (HeLa) and p=0.0166 (SiHa). HeLa and SiHa cells were transfected with si-NC, si-GOLPH3, oe-vector, or oe-GOLPH3 for 48 h. B) The levels of NRF2 in cytoplasm and nucleus were determined by western blot. NRF2 in nucleus: si-NC vs. si-GOLPH3: p=0.0011 (HeLa) and p=0.0034 (SiHa), oe-vector vs. oe-GOLPH3: $p < 0.0001$ (HeLa) and $p < 0.0001$ (SiHa). The transfected cells were pretreated with or without 10 μM SC79 for 1 h. C) The protein levels of p-AKT and AKT were evaluated by western blot. For p-AKT/AKT: si-NC vs. si-GOLPH3: p=0.0335 (HeLa) and p=0.0026 (SiHa), si-GOLPH3 vs. si-GOLPH3+SC79: p=0.0031 (HeLa) and p=0.0086 (SiHa). The transfected cells were treated with 10 μM erastin for 24 h and with 10 μM SC79 for 1 h. D) Cell viability was assessed by CCK-8 assay. si-NC+erastin vs. si-GOLPH3+erastin: p=0.0040 (HeLa) and p=0.0015 (SiHa), si-GOLPH3+erastin vs. si-GOLPH3+SC79+erastin: p=0.0055 (HeLa) and p=0.0043 (SiHa). E) Cell proliferation was measured by colony formation assay. si-NC+erastin vs. si-GOLPH3+erastin: p=0.0044 (HeLa) and

Accepted manuscript

p=0.0001 (SiHa), si-GOLPH3+erastin vs. si-GOLPH3+SC79+erastin: p=0.0206 (HeLa) and p=0.0001 (SiHa). F) Lipid peroxidation levels were detected using C11-BODIPY fluorescent probe via flow cytometry. si-NC+erastin vs. si-GOLPH3+erastin: p=0.0139 (HeLa) and p=0.0003 (SiHa), si-GOLPH3+erastin vs. si-GOLPH3+SC79+erastin: p=0.0133 (HeLa) and p=0.0003 (SiHa). G) MDA content was measured by commercial kit. si-NC+erastin vs. si-GOLPH3+erastin: p=0.0029 (HeLa) and p=0.0042 (SiHa), si-GOLPH3+erastin vs. si-GOLPH3+SC79+erastin: p=0.0173 (HeLa) and p=0.0046 (SiHa). All experiments were conducted in three independent biological replicates. n=3. *p < 0.05, **p < 0.01, ***p < 0.001

Figure 4. NSUN2 mediated the m^5 C modification of GOLPH3 and increased its stability. A) Correlation between NSUN2 and GOLPH3 expression in CESC from the starBase database was analyzed. B) The m^5 C modification level on GOLPH3 mRNA in CC cells was validated by MeRIP assay. For HeLa, IgG vs. m^5 C: p=0.0002; for SiHa, IgG vs. m^5 C: p=0.0002. C) The binding between NSUN2 and GOLPH3 mRNA in CC cells was verified by RIP assay. For HeLa, IgG vs. NSUN2: p < 0.0001; for SiHa, IgG vs. NSUN2: p=0.0001. CC cells were transfected with si-NC or si-NSUN2 for 48 h. D, E) NSUN2 and GOLPH3 were detected by RT-qPCR and western blot, respectively. For NSUN2 mRNA, si-NC vs. si-NSUN2: p=0.0003 (HeLa) and p=0.0014 (SiHa); for GOLPH3 mRNA, si-NC vs. si-NSUN2: p=0.0011 (HeLa) and p=0.0009 (SiHa); for NSUN2 protein, si-NC vs. si-NSUN2: p < 0.0001 (HeLa) and p=0.0033 (SiHa); for GOLPH3 protein, si-NC vs. si-NSUN2: p=0.0008 (HeLa) and p=0.0053 (SiHa). F) The m^5 C modification level on GOLPH3 mRNA was measured by MeRIP assay. For HeLa: si-NC vs. si-NSUN2: p=0.0005, for SiHa: si-NC vs. si-NSUN2: p=0.0013. G) GOLPH3 mRNA stability was assessed by RT-qPCR after Actinomycin D (5 μg/ml) for 0, 2 and 4 h. For HeLa: si-NC vs. si-NSUN2: p=0.0015, for SiHa: si-NC vs. si-NSUN2: p=0.0020. All experiments were conducted in three independent biological replicates. n=3. **p < 0.01, ***p < 0.001

Figure 5. ALYREF was implicated in the NSUN2-mediated GOLPH3 mRNA stability. A) The binding between ALYREF and GOLPH3 mRNA in CC cells was measured by RIP assay. For HeLa, IgG vs. ALYREF: p=0.0001; for SiHa, IgG vs. ALYREF: p < 0.0001. CC cells underwent

Accepted manuscript

transfection with si-NC or si-ALYREF for 48 h. B, C) ALYREF and GOLPH3 levels were examined by RT-qPCR and western blot, respectively. For ALYREF mRNA, si-NC vs. si-ALYREF: p=0.0001 (HeLa) and p=0.0006 (SiHa); for GOLPH3 mRNA, si-NC vs. si-ALYREF: p=0.0039 (HeLa) and p=0.0037 (SiHa); for ALYREF protein, si-NC vs. si-ALYREF: p=0.0084 (HeLa) and p=0.0003 (SiHa); for GOLPH3 protein, si-NC vs. si-ALYREF: p=0.0113 (HeLa) and p=0.0014 (SiHa). D) GOLPH3 mRNA stability was evaluated by RT-qPCR after 5 μg/ml Actinomycin D for 0, 2 and 4 h. For HeLa: si-NC vs. si-ALYREF: p=0.0017, for SiHa: si-NC vs. si-ALYREF: p=0.0112. CC cells were transfected with si-NSUN2 and/or oe-ALYREF for 48 h. E) ALYREF and GOLPH3 mRNA levels were measured by RT-qPCR. For ALYREF mRNA, si-NC+oe-vector vs. si-NC+oe-ALYREF: $p < 0.0001$ (HeLa) and $p < 0.0001$ (SiHa); si-NSUN2+oe-vector vs. si-NSUN2+oe-ALYREF: $p < 0.0001$ (HeLa) and $p < 0.0001$ (SiHa); for GOLPH3 mRNA, si-NC+oe-vector vs. si-NSUN2+oe-vector: p=0.0004 (HeLa) and p=0.0011 (SiHa); si-NC+oe-vector vs. si-NC+oe-ALYREF: $p < 0.0001$ (HeLa) and $p < 0.0001$ (SiHa); si-NSUN2+oe-vector vs. si-NSUN2+oe-ALYREF: p=0.0264 (HeLa) and p=0.0443 (SiHa); si-NC+oe-ALYREF vs. si-NSUN2+oe-ALYREF: $p < 0.0001$ (HeLa) and $p < 0.0001$ (SiHa). F) ALYREF and GOLPH3 protein levels were measured by western blot. For ALYREF protein, si-NC+oe-vector vs. si-NC+oe-ALYREF: p=0.0074 (HeLa) and p=0.0007 (SiHa); si-NSUN2+oe-vector vs. si-NSUN2+oe-ALYREF: p=0.0034 (HeLa) and p=0.0015 (SiHa); for GOLPH3 protein, si-NC+oe-vector vs. si-NSUN2+oe-vector: p=0.0002 (HeLa) and p=0.0014 (SiHa); si-NC+oe-vector vs. si-NC+oe-ALYREF: p=0.0006 (HeLa) and p=0.0025 (SiHa); si-NSUN2+oe-vector vs. si-NSUN2+oe-ALYREF: p=0.0051 (HeLa) and p=0.0320 (SiHa); si-NC+oe-ALYREF vs. si-NSUN2+oe-ALYREF: $p < 0.0001$ (HeLa) and p=0.0002 (SiHa). G) GOLPH3 mRNA stability was determined by RT-qPCR after Actinomycin D (5 μg/ml) for 0, 2 and 4 h. si-NC+oe-vector vs. si-NSUN2+oe-vector: p=0.0484 (HeLa) and p=0.0216 (SiHa); si-NC+oe-vector vs. si-NC+oe-ALYREF: p=0.0005 (HeLa) and p=0.0033 (SiHa); si-NSUN2+oe-vector vs. si-NSUN2+oe-ALYREF: p=0.0300 (HeLa) and p=0.0370 (SiHa); si-NC+oe-ALYREF vs. si-NSUN2+oe-ALYREF: p=0.0007 (HeLa) and p=0.0021 (SiHa). All experiments were conducted in three independent biological replicates. n=3. *$p < 0.05$, **$p < 0.01$, ***$p < 0.001$

Accepted manuscript

Figure 6. The combination of NSUN2 siRNA and cisplatin inhibited CC cell growth by enhancing ferroptosis via GOLPH3 suppression. CC cells were transfected with si-NSUN2 alone or together with oe-GOLPH3 for 48 h. A) NSUN2 and GOLPH3 levels were detected by western blot. For NSUN2 protein, si-NC vs. si-NSUN2: p=0.0001 (HeLa) and p=0.0039 (SiHa); for GOLPH3 protein, si-NC vs. si-NSUN2: p=0.0001 (HeLa) and p=0.0005 (SiHa); si-NSUN2+oe-vector vs. si-NSUN2+oe-GOLPH3: p=0.0003 (HeLa) and p=0.0008 (SiHa). Following 48 h of transfection with si-NSUN2 alone or co-transfection with oe-GOLPH3, CC cells were exposed to cisplatin at 10 μg/ml (SiHa cells) or 5 μg/ml (HeLa cells) for 24 h. B) Cell viability was assessed by CCK-8 assay. si-NC+cisplatin vs. si-NSUN2+cisplatin: p=0.0009 (HeLa) and p=0.0018 (SiHa); si-NSUN2+oe-vector+cisplatin vs. si-NSUN2+oe-GOLPH3+cisplatin: p=0.0097 (HeLa) and p=0.0027 (SiHa). C) Cell proliferation was measured by colony formation assay. si-NC+cisplatin vs. si-NSUN2+cisplatin: p=0.0018 (HeLa) and $p < 0.0001$ (SiHa); si-NSUN2+oe-vector+cisplatin vs. si-NSUN2+oe-GOLPH3+cisplatin: p=0.0012 (HeLa) and p=0.0002 (SiHa). D) Lipid peroxidation levels were detected using C11-BODIPY fluorescent probe via flow cytometry. si-NC+cisplatin vs. si-NSUN2+cisplatin: p=0.0011 (HeLa) and p=0.0004 (SiHa); si-NSUN2+oe-vector+cisplatin vs. si-NSUN2+oe-GOLPH3+cisplatin: p=0.0010 (HeLa) and p=0.0004 (SiHa). E) MDA content was measured by commercial kit. si-NC+cisplatin vs. si-NSUN2+cisplatin: p=0.0186 (HeLa) and p=0.0008 (SiHa); si-NSUN2+oe-vector+cisplatin vs. si-NSUN2+oe-GOLPH3+cisplatin: p=0.0408 (HeLa) and p=0.0066 (SiHa). All experiments were conducted in three independent biological replicates. n=3. $*p < 0.05$, $**p < 0.01$, $***p < 0.001$

Accepted manuscript

Fig. 1 Download full resolution image

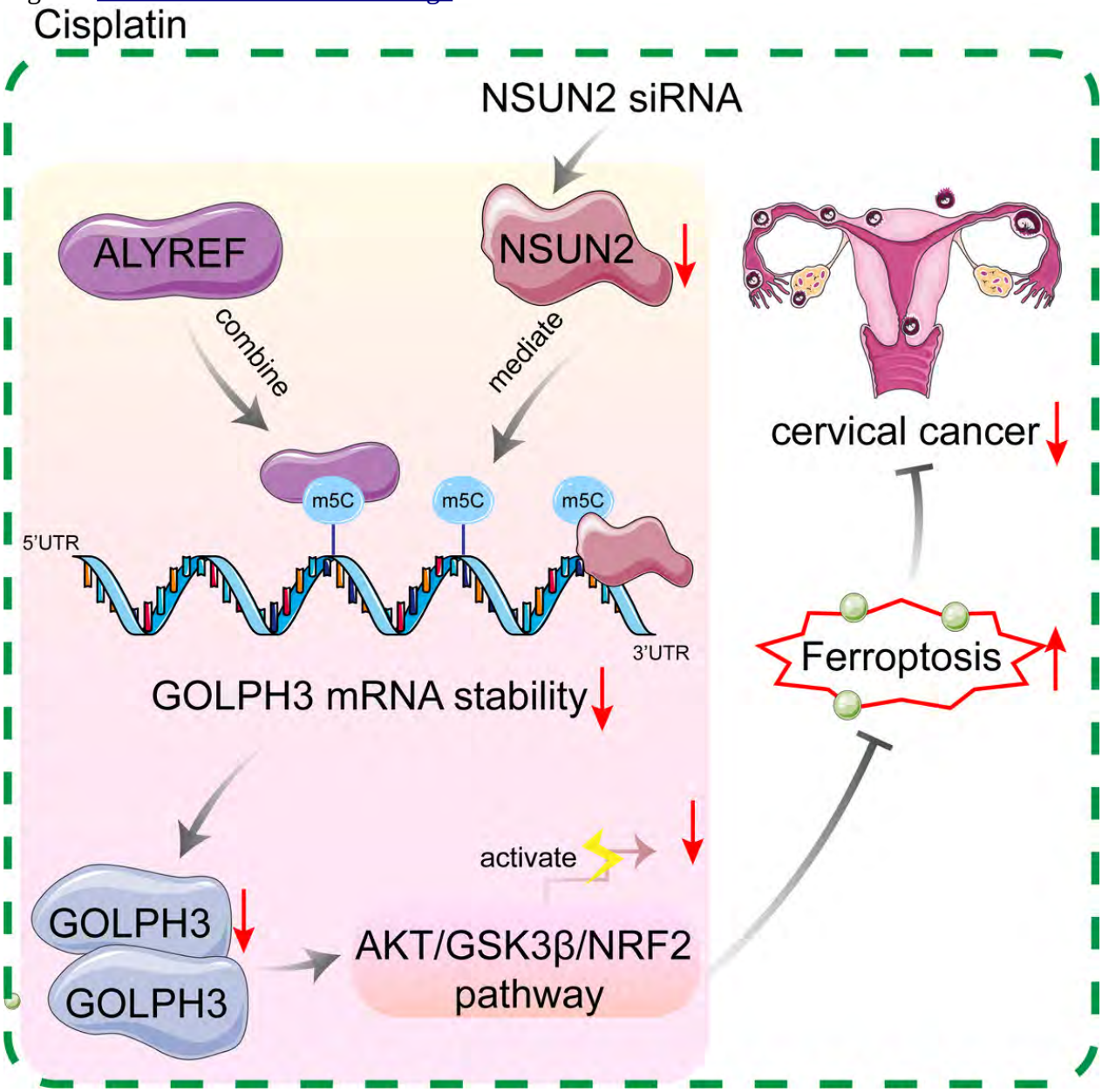

Fig. 2 [Download full resolution image]

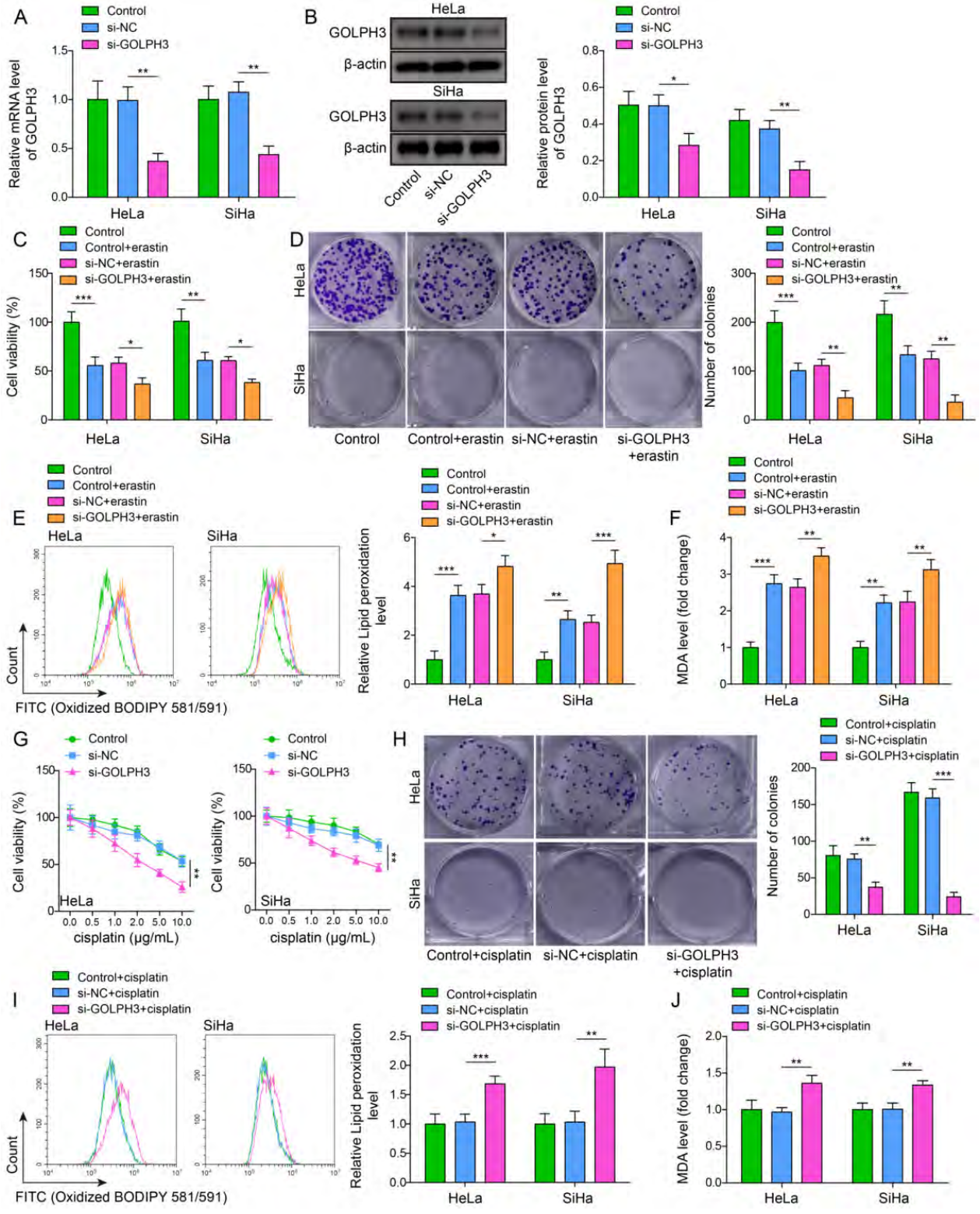

Fig. 3 [Download full resolution image]

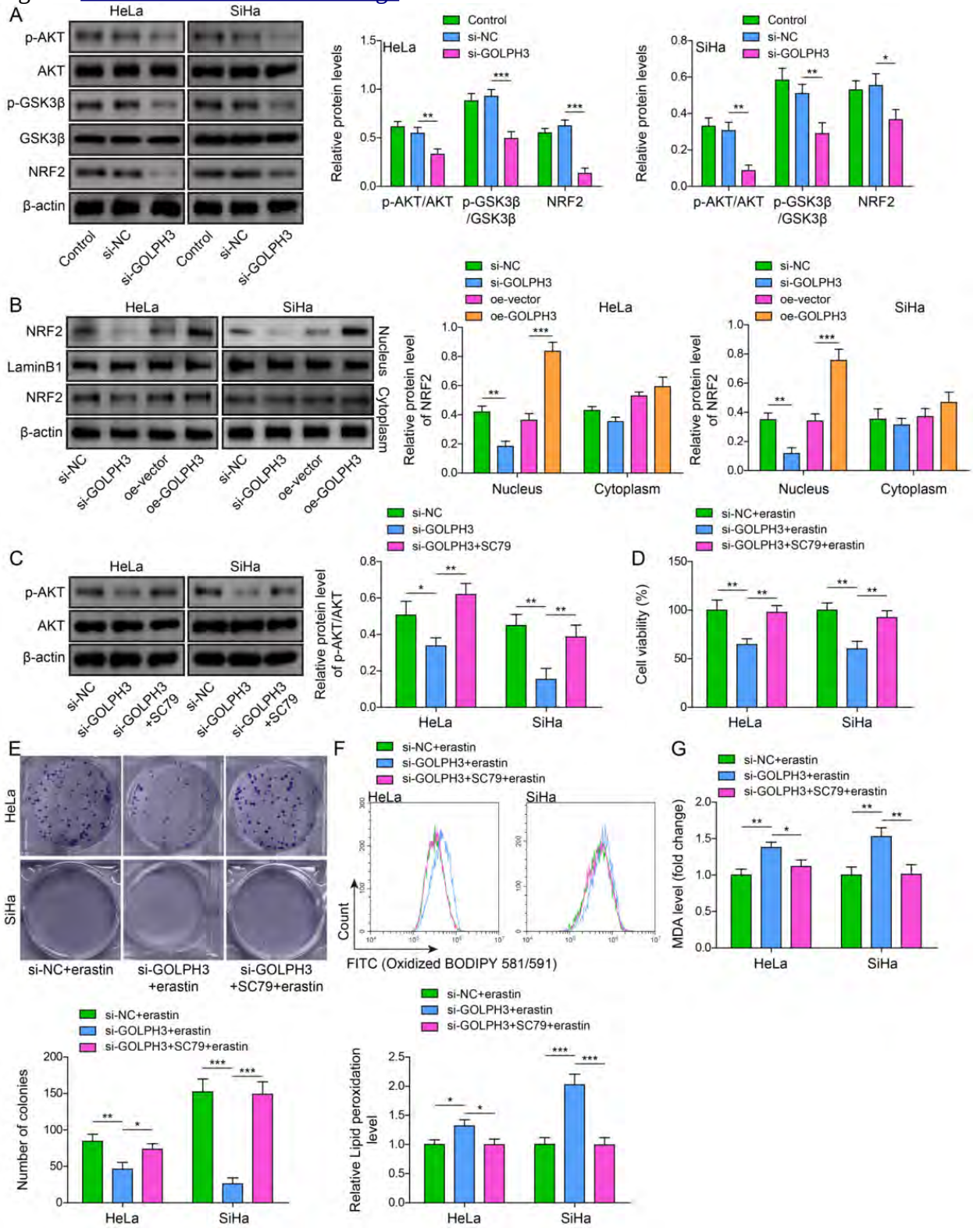

Fig. 4 [Download full resolution image]

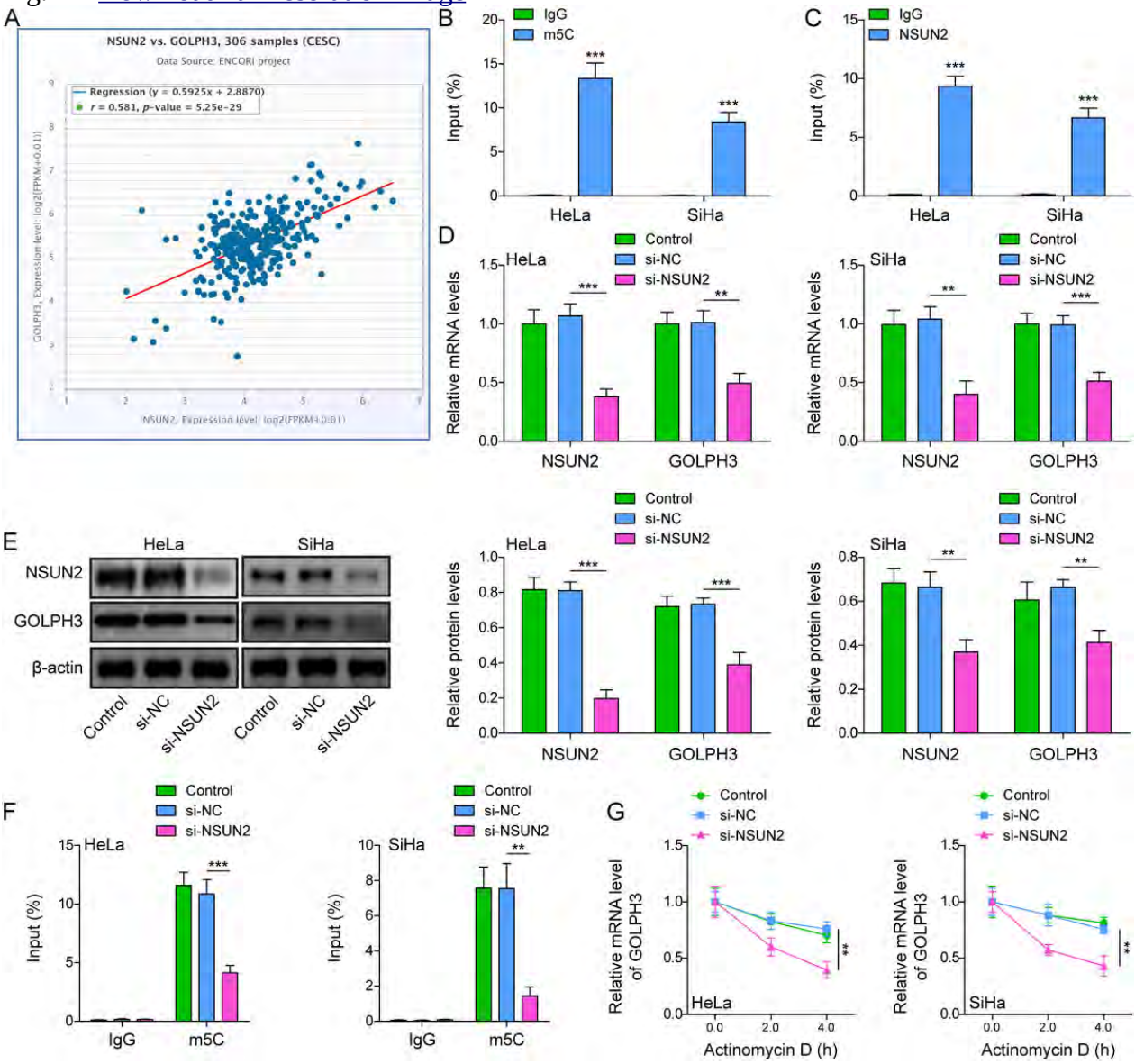

Fig. 5 Download full resolution image

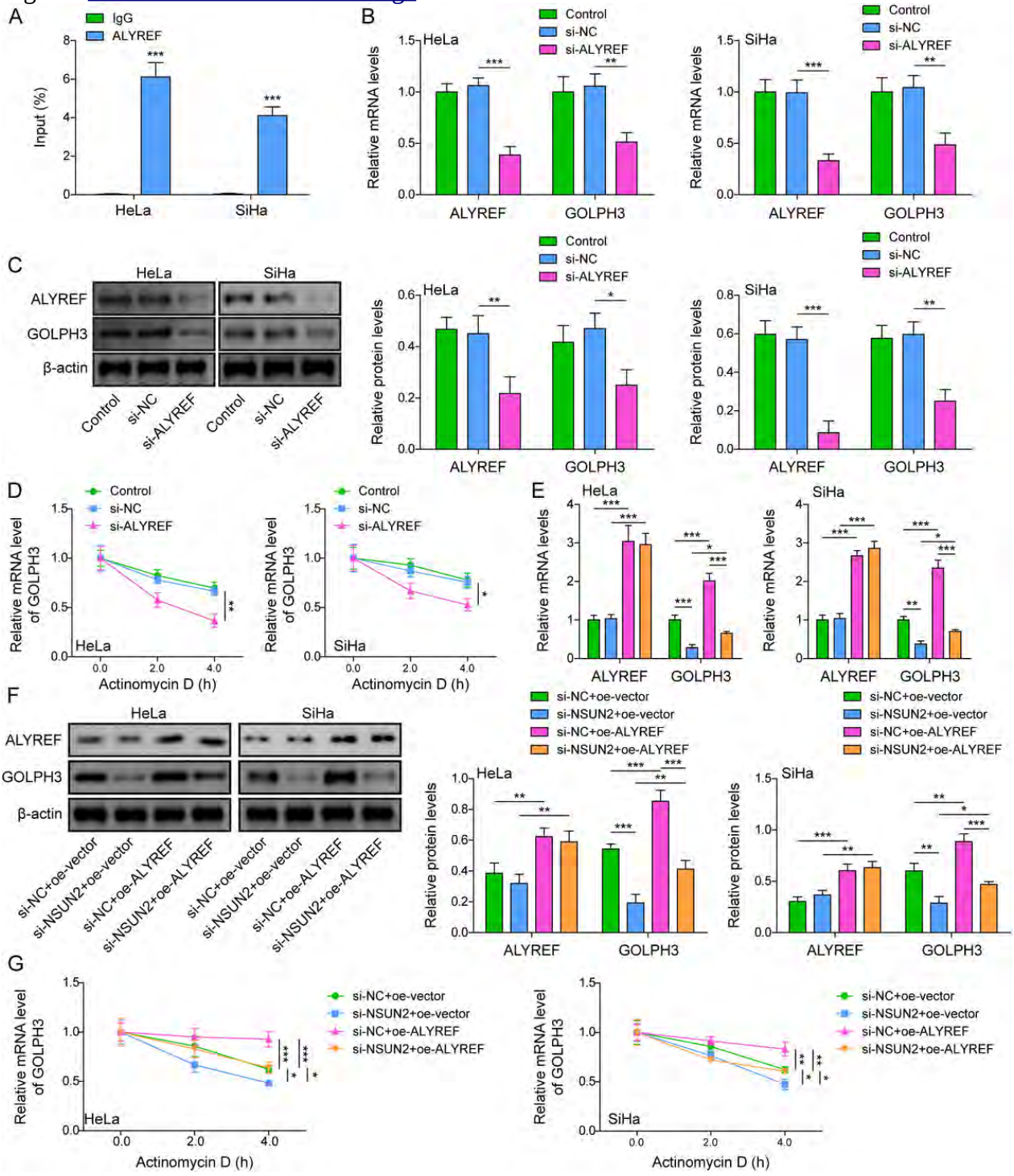

Fig. 6 [Download full resolution image]

